Catalysis Today 179 (2012) 43–51

Contents lists available at ScienceDirect

Catalysis Today

journal homepage: www.elsevier.com/locate/cattod

Study of the interaction between components in hybrid CuZnAl/HZSM-5 catalysts and its impact in the syngas-to-DME reaction

A. García-Trenco, A. Vidal-Moya, A. Martínez*

Instituto de Tecnología Química UPV-CSIC, Av. de los Naranjos s/n, 46022 Valencia, Spain

ARTICLE INFO

Article history:
Received 30 May 2011
Accepted 15 June 2011
Available online 28 July 2011

Keywords:
Synthesis gas
Methanol dehydration
Dimethyl ether
Hybrid catalyst
CuZnAl
ZSM-5 zeolite
Detrimental interactions
EPR spectroscopy

ABSTRACT

Hybrid CuZnAl(CZA)/HZSM-5 catalysts were prepared by three mixing methods in order to analyze the possible existence of interactions between components and their impact in the STD process, namely: (a) grinding of powders prior to pelletizing (grinding method), (b) slurrying the two solids in water followed by drying and pelletizing (slurry method), and (c) physical mixture of pre-pelletized components. The materials were characterized by ICP-OES, XRD, N_2 physisorption, H_2-TPR, ^{27}Al MAS NMR, FTIR-pyridine, and EPR spectroscopy. Detrimental interactions producing a drastic reduction in the amount of available zeolitic Brønsted acid sites were observed for the hybrids prepared by slurry and grinding methods. Such interactions involved, on one hand, the partial blockage of micropores by CZA particles and, on the other hand, an inter-cationic exchange of Cu^{2+} (and possibly also Zn^{2+}) species. The presence of isolated Cu^{2+} cations occupying exchange positions in the HZSM-5 zeolite was unambiguously evidenced by EPR spectroscopy. The decrease in Brønsted acidity significantly reduced the activity of the zeolite for dehydrating methanol leading to a much lower efficiency of the corresponding hybrids for DME synthesis at typical STD conditions as compared to the catalyst obtained by simple mixture of pre-pelletized components.

1. Introduction

Dimethyl ether (DME) is an important intermediate for the production of useful chemicals (i.e. methyl acetate and dimethyl sulfate) and petrochemicals (light olefins, BTX aromatics) [1,2]. Recently, DME has also been considered as an ideal eco-friendly substitute for conventional petroleum-derived diesel owing to its high cetane number (55–60), low auto-ignition temperature, lower emissions of toxic compounds upon combustion, and reduced noise [3,4]. DME is traditionally produced by a two-step process involving first the synthesis of methanol from syngas on a Cu-based catalyst followed by the dehydration of methanol in the presence of a solid acid catalyst. Though the syngas feeding the methanol synthesis reactor is typically obtained from fossil resources such as coal, natural gas and crude oil, the production of DME from biomass-derived syngas (the so-called bioDME) is particularly attractive as in this case it can be considered as a carbon-neutral fuel from the viewpoint of CO_2 emissions thus contributing to restrain the global warming effect caused by the emission of greenhouse gases. The increasing interest in using DME (and particularly bioDME) as an environmentally benign diesel fuel has promoted extensive research in the so-called STD (syngas-to-DME) process in which DME is produced directly from syngas in a single catalytic reactor with the corresponding costs savings [5,6]. A salient advantage of the STD route is that, by rapidly consuming in situ the formed methanol, it allows overcoming the thermodynamic constraints of the methanol synthesis reaction allowing much higher per-pass CO conversions (and thus DME yields) to be attained as compared to the conventional two-step process. This can be easily inferred by looking to the main four reactions involved in the STD process described by the following Eqs. (1)–(4):

$$2CO + 4H_2 \leftrightarrow 2CH_3OH \quad (1)$$

$$CO_2 + 3H_2 \leftrightarrow CH_3OH + H_2O \quad (2)$$

$$2CH_3OH \leftrightarrow CH_3OCH_3 + H_2O \quad (3)$$

$$H_2O + CO \leftrightarrow H_2 + CO_2 \quad (4)$$

According to this set of reactions the product of one reaction is the reactant for another thus creating a synergistic effect that shifts the equilibrium of the methanol synthesis reactions (1) and (2) to the right.

It is clear from the above set of reactions that a suitable STD catalyst should combine two catalytic functionalities in order to effectively couple the methanol synthesis and methanol dehydration reactions. Typically, the methanol synthesis function is provided by a Cu-based catalyst (e.g. $CuO/ZnO/Al_2O_3$, abbreviated as CuZnAl) while the dehydration of methanol to DME is afforded by a solid acid component such as γ-Al_2O_3 or zeolites [7–12]. Among

* Corresponding author.
E-mail address: amart@itq.upv.es (A. Martínez).

0920-5861/$ – see front matter © 2011 Elsevier B.V. All rights reserved.
doi:10.1016/j.cattod.2011.06.034

the zeolites, most of the studies were focused on the medium-pore HZSM-5 [7–9,12,13] as the size of its pores prevents extensive coking without severely hindering the diffusion of the molecules involved in the DME synthesis, although other zeolitic structures such as ferrierite [14,15], mordenite [13], and HY [10,15], as well as SAPO-*x* zeotypes [16] have also been explored. In general, zeolites are preferred over alumina since the much higher dehydration activity of the former (owing to a substantially higher acidity) allows for performing the STD reaction at lower temperatures and thus under thermodynamically more favorable conditions for the methanol synthesis step. Higher reaction temperatures do also tend to favor secondary reactions leading to hydrocarbons in detriment of DME and to carbon deposits that negatively impact the catalyst lifetime.

In order to attain a good synergy between the main reactions involved in the STD process and thus to maximize the DME formation rate, it seems reasonable *a priori* that the preparation of the bifunctional STD catalyst should target a close proximity between the active sites of the two catalytic functions as, in fact, it has been predicted in a reactor simulation study [17]. However, while being conceptually correct, earlier studies have clearly shown that the employment of preparation methodologies favoring a closer contact between components in hybrid CuO/ZnO/γ-Al_2O_3 catalysts (where γ-Al_2O_3 provides the methanol dehydration function) does not necessarily produce the most efficient STD catalysts [10,11,18]. A similar conclusion was drawn for CuZnAl/SiO_2–Al_2O_3 catalysts prepared using different strategies leading to different degrees of intimacy between components [19]. It is learned from these studies that the use of preparation methods, such as coprecipitation–impregnation, coprecipitation–sedimentation, sol–gel impregnation, or the simplest (and most widely applied) physical mixture of the two components, in where the active sites for the methanol synthesis and methanol dehydration functions are formed in separated stages, leads to more effective hybrid catalysts than when the active sites are generated from a common Cu–Zn–Al coprecipitate, even if the last approach is that conducting to a more intimate contact between components. This behavior may be accounted for by considering the existence of detrimental interactions between the two catalytic functions in intimate contact worsening the overall STD performance. Detrimental interactions between the methanol synthesis and dehydration functions may not only take place at the catalyst preparation and/or activation stages, as it is inferred from the above examples, but also they have been shown to occur during the liquid phase DME synthesis in slurry-type reactors (LPDME process) [20]. In this later case, based on SEM–EDS analyses of a spent CuO/ZnO/γ-Al_2O_3 hybrid catalyst prepared by physical mixture of the individual component powders, the interaction was suggested to occur by the migration of Cu- and Zn-containing species from the methanol catalyst to the alumina poisoning the acid sites active for methanol dehydration [20]. Nevertheless, due to the poor signal-to-noise ratio in the SEM–EDS measurements, a definitive conclusion regarding the *inter-catalyst migration* hypothesis as the likely interaction mechanism could not be made [20].

As mentioned previously, the most extended methodology for preparing hybrid STD catalysts, particularly for those comprising zeolites as the dehydration function, is the simple physical mixture of the individual components. In fact, a significant blockage of the zeolite micropores by the methanol synthesis component has been observed in hybrid Cu–Zn(–Al)/H-ferrierite catalysts prepared by coprecipitation–impregnation or coprecipitation–sedimentation methods [21,22]. However, even for catalysts prepared by physical mixture, it appears that detrimental interactions might also occur depending on the specific mixing method employed. For instance, Takeguchi et al. [23] reported that a Cu–Zn–Ga/silica–alumina catalyst prepared by mixing the previously pelletized components is more active for the syngas-to-DME reaction than the equivalent catalyst obtained by milling (grinding) the two component powders prior to pelletizing. The authors attributed this fact to the masking of active sites in the methanol synthesis component by the silica–alumina particles at the mixing and tabletting stages of the grinding approach, though no experimental proofs other than the different catalytic behaviors were presented.

Despite the above discussions clearly highlight the importance of the possible existence of detrimental interactions between components in hybrid STD catalysts (even in those prepared by the most common physical mixture approach) no much effort has been devoted in the previous literature to this issue. To the best of our knowledge, there are no previous studies aimed at addressing interaction effects in hybrid STD catalysts comprising zeolites as the dehydration component. In the present work we provide, for the first time, experimental evidences based on EPR characterization that such detrimental interactions may take place in hybrid CuZnAl/HZSM-5 catalysts depending on the mixing method used. The consequences of such interactions on the activity of the two catalytic functions are also addressed.

2. Experimental

2.1. Preparation of catalysts

A CuO–ZnO–Al_2O_3 methanol synthesis catalyst precursor with a nominal Cu:Zn:Al atomic ratio of 6:3:1 was prepared by coprecipitation following the optimized procedure reported in [24]. Specifically, an aqueous solution containing the respective metal nitrates [$Cu(NO_3)_2$ (0.6 M), $Zn(NO_3)_2$ (0.3 M), and $Al(NO_3)_3$ (0.1 M)] and an aqueous solution of Na_2CO_3 (1 M) as precipitating agent were simultaneously added at a rate of 5 mL/min to a glass beaker kept under stirring at 70 °C and a constant pH of 7.0. After the addition was completed, the suspension was aged for 1 h at the above conditions and the resulting precipitate was then filtered, exhaustively washed with deionized water, dried at 100 °C for 12 h, and finally calcined under a flow of air (25 mL/min) at 300 °C for 3 h. The methanol synthesis precursor so obtained is denoted here as CZA.

A commercial ZSM-5 zeolite (CBV8020, Zeolyst International, nominal Si/Al = 40) in its protonic form (sample denoted here as HZ) was used as the methanol dehydration function. Then, three different mixing methods were adopted in order to prepare the hybrid CZA/HZ samples: (a) addition of dry powders of the two components to a beaker containing deionized water at ambient temperature and stirring of the slurry for 30 min, followed by separation of the solid mixture by filtration, drying at 100 °C overnight, and pelletizing (hereinafter denoted as slurry method); (b) careful grinding of the individual component powders in an agate mortar for 15 min followed by pelletizing of the formed homogeneous solid mixture (denoted here as grinding method); and (c) simple physical mixture of the two pre-pelletized components. In all cases, catalysts pellets of 0.25–0.42 mm were used for the catalytic studies. Using the above three methods a series of hybrid CZA:HZ catalysts with variable mass ratios between components were produced for different characterization and catalytic purposes, as will be explained along the work. The hybrid catalysts were designated as CZA/HZ(*x*)Y, where *x* is the CZA:HZ mass ratio and Y is S, G, or M and refers to the mixing method used, i.e. S = slurry, G = grinding, and M = mixture of pellets.

In order to address how the mixing method applied affected the activity of the CZA component for the synthesis of methanol from syngas, mixtures of CZA with silicalite-1 (the pure silica MFI counterpart, abbreviated as S1) were prepared in a CZA:S1 mass ratio of 2:1 by the same three methods used for producing the CZA/HZ hybrids. The CZA/S1 mixtures were denoted as CZA/S1(2:1)Y (Y = S,

G, or M). The acid-free silicalite-1 sample was hydrothermally synthesized as reported in [25]. Briefly, a gel with the molar composition 9TPAOH:0.16NaOH:25SiO_2:495H_2O:100EtOH was prepared using TEOS as the silica source, transferred to a Teflon-lined stainless steel autoclave and crystallized at 160 °C for 48 h in static conditions. Subsequently, the solid was recovered after several cycles of centrifuging and washing with deionized water until a pH of 7 in the washing waters was attained, dried at 100 °C in an oven overnight, and finally calcined at 600 °C for 10 h to remove the organic material.

2.2. Characterization techniques

The chemical composition of the methanol synthesis component (Cu/Zn/Al atomic ratio) and the HZSM-5 zeolite (Si/Al ratio) was determined by Inductively Coupled Plasma-Optical Emission Spectroscopy (ICP-OES) in a Varian 715-ES apparatus after dissolution of the solids in an acid mixture of HNO_3:HF:HCl in a 1:1:3 volume ratio.

The identification of crystalline phases in the calcined CZA precursor and hybrid CZA/HZ catalysts prepared by different mixing methods as well as the phase purity of the home-made silicalite-1 sample were ascertained by powder X-ray diffraction (XRD). XRD patterns were recorded on a PANanalytical Cubix Pro diffractometer equipped with a graphite monochromator operating at 40 kV and 45 mA using nickel-filtered Cu K_α radiation (λ = 0.1542 nm). The average crystallite size of the CuO phase in calcined CZA and CZA/HZ hybrids was estimated by applying the Scherrer's equation to the most intense CuO peak at 38.8° (2θ) corresponding to the (1 1 1) reflection.

Textural properties were determined by N_2 adsorption at −196 °C in a Micromeritics ASAP 2000 equipment. The specific surface area was calculated following the BET method and the micropore volume using the *t*-plot approach. Prior to the adsorption measurements, the samples were degassed at 200 °C (calcined CZA precursor and CZA/HZ hybrids) or 400 °C (HZSM-5 and silicalite-1) under vacuum for 24 h. The use of a lower degassing temperature in the case of CZA and CZA/HZ samples is advised in order to prevent the advent of irreversible structural changes that may occur in the CZA catalyst when heated at temperatures above 300 °C (in fact, the calcination temperature employed here to generate the oxides in the CZA precursor) [24].

The acidity of the samples was measured by infrared spectroscopy coupled with the adsorption of pyridine in a Nicolet 710 FTIR apparatus. Self-supported wafers of 10 mg/cm^2 were previously degassed at 260 °C overnight under dynamic vacuum (10^{-4} Pa). Then, 1.8×10^3 Pa of pyridine were admitted to the IR cell and, after equilibration at ambient temperature, the sample was degassed for 1 h at 250 °C, the spectrum recorded at room temperature, and the background subtracted. The amounts of Brønsted and Lewis acid sites were determined from the integrated areas of the IR pyridine bands at ca. 1545 and 1450 cm^{-1}, respectively, using the extinction coefficients reported by Emeis [26].

The reduction behavior of the calcined CZA precursor and CZA/HZ hybrids (CZA:HZ mass ratio of 2:1) was studied by H_2-TPR in a Micromeritics Autochem 2910 equipment. About 30 mg of sample were initially flushed with Ar at room temperature for 30 min. Then, the gas was switched to the reductive mixture of 10 vol% H_2 in Ar (flow rate = 50 mL/min) and the temperature linearly increased from ambient till 600 °C at a heating rate of 10 °C/min. Water formed in the reduction was retained in a 2-propanol/$N_{2(l)}$ trap and the H_2 consumption rate was monitored in a thermal conductivity detector (TCD) previously calibrated using the reduction of CuO as a reference.

The ^{27}Al MAS NMR spectra were recorded at ambient temperature in a Bruker AV-400 WB spectrometer using a BL4 mm probe, a magnetic field of 9.4 T, a spinning rate of 10 kHz, and a recycle delay of 0.5 s. ^{27}Al chemical shifts were referred to $Al(NO_3)_3$.

The electron paramagnetic resonance (EPR) spectroscopic measurements were performed in a Bruker EMX-12 equipment at 100 K working at the X-band (9.46 GHz), with a field modulation frequency of 100 kHz and modulation amplitude of 1.0 G. The concentration of paramagnetic species was calculated by double integration of the first derivative spectra, using copper sulfate as a calibration standard.

2.3. Catalytic experiments

Different types of catalytic experiments were performed in order to assess the impact of the mixing method applied in the preparation of the hybrid CZA/HZ catalysts on the activity of the two catalytic functions, i.e. methanol synthesis (on the CZA component) and methanol dehydration (on the zeolite).

2.3.1. Dehydration of pure methanol

The activity for dehydration of anhydrous methanol (99.8% purity, Sigma–Aldrich) of the HZSM-5 zeolite was determined in a fixed bed continuous-flow quartz reactor loaded with 15 mg of the zeolite previously diluted with 2 mL of inert SiC. The dehydration experiments were performed at 260 °C (that is, the same reaction temperature applied in the STD runs) and atmospheric pressure by feeding a gas mixture consisting of 20 mol% MeOH in N_2 at a total flow rate of 150 mL/min. The composition of the reactor effluent was determined at regular time intervals on line in a gas chromatograph (HP-GC6890) equipped with a TBR-5 capillary column and a FID-type detector. The reported reaction rates correspond to the *pseudo*-steady state (TOS ca. 2 h).

In order to assess whether or not the mixing method applied for the preparation of the CZA/HZ hybrids have an influence on the dehydration activity of the zeolite component, the original HZ sample was submitted to the following two treatments simulating the conditions in the slurry and grinding methods. Thus, the conditions in the slurry method were approached by immersing the zeolite powder in a beaker containing deionized water and agitation of the slurry for 30 min at room temperature, followed by filtration and drying at 100 °C (sample denoted as HZS). On the other hand, the grinding method was simulated by grinding the zeolite powder in an agate mortar for 15 min, thus producing sample HZG.

2.3.2. Syngas-to-DME (STD) experiments

The STD experiments were carried out in a down-flow fixed bed stainless-steel reactor. Typically, the reactor was loaded with 0.8 g of catalyst previously diluted with SiC (total bed volume of 10 mL). Prior to feeding syngas the catalyst was reduced by flowing 120 mL/min of diluted hydrogen (5 vol% H_2 in N_2) through the reactor at atmospheric pressure and 245 °C (2 °C/min) for 10 h. Subsequently, the temperature in the catalyst bed was lowered to 85 °C under the flow of diluted H_2 and the reductive gas replaced by a mixture of 90 vol% syngas/10 vol% Ar (Ar used as internal standard for GC analyses) with the syngas having the molar composition of 66%H_2/30%CO/4%CO_2. Once the syngas/Ar flow was established, the reactor pressure was set to 4.0 MPa and the temperature increased up to the reaction temperature of 260 °C at a rate of 4 °C/min. The reaction was conducted at the above conditions for about 6 h. No significant deactivation of the catalysts was observed in this period. The product stream leaving the reactor was depressurized and analyzed on line at different time intervals in a Varian 450-GC gas chromatograph equipped with a TCD for the separation and quantification of CO, CO_2, and Ar, and a FID for the analysis of oxygenates (mostly MeOH and DME) and hydrocarbons. The lines connecting the reactor outlet with the GC injection valve were kept at 180 °C during the run so as to avoid any product condensation. Product

yields and selectivities are given and on a carbon basis. The catalytic data reported here correspond to a time-on-stream (TOS) of ca. 3 h as representative of the *pseudo*-steady state.

Using the above reactor setup and general reaction conditions, three types of experiments were performed. In one of them the reactor was loaded with acid-free CZA/S1 mixtures (CZA:S1 mass ratio of 2:1, see Section 2.1 for further preparation details) with the aim of determining exclusively the influence of the mixing method on the methanol synthesis activity of the CZA component. In this case, the syngas conversion runs were done at a constant gas-hourly-space-velocity (GHSV) of 15.0 $L_{syngas}\ g_{cat}^{-1}\ h^{-1}$ in order to obtain CO conversions below the equilibrium conversion at the studied conditions ($X_{CO\text{-}equil} \approx 38\%$). The second set of experiments was also aimed at determining the activity of the CZA component for synthesis of methanol in the acid-containing CZA/HZ hybrids. For this purpose, the hybrids with a CZA:HZ mass ratio of 2:1 (thus with "excess" acid sites) were used and the STD runs were performed at different GHSV values in the range of 1.7–8.5 $L_{syngas}\ g_{cat}^{-1}\ h^{-1}$ so as the overall STD reaction becomes controlled by the methanol synthesis reaction. The third type of STD experiments was targeted at addressing the impact of the preparation method on the zeolite dehydration activity. In this case the STD experiments were run under methanol dehydration-controlled conditions (thus, with "defect" of acid sites) using hybrid catalysts with higher CZA:HZ mass ratios of 3:1 and 6:1. The runs were conducted at a constant GHSV of 1.7 $L_{syngas}\ g_{cat}^{-1}\ h^{-1}$.

3. Results and discussion

3.1. Characterization of materials

The Cu:Zn:Al atomic ratio in the calcined CZA catalyst as determined by ICP-OES was 6.0Cu:2.9Zn:1.1Al, in very good agreement with the nominal atomic ratio of 6.0:3.0:1.0 expected from the metal concentrations used in the respective nitrate precursor solutions. The actual Si/Al ratio in the HZSM-5 sample was 32.3, a value slightly lower than the nominal ratio of 40 given by the supplier.

The silicalite-1 sample synthesized in this work exhibited very high crystallinity and MFI phase purity, as inferred from the XRD pattern of the calcined material (see Fig. S1 of Supporting information). Moreover, the calcined silicalite-1 displayed a BET area of 385 m^2/g and a micropore volume of 0.172 mL/g which are fully consistent with reported values [25].

The XRD of the calcined CZA precursor is shown in Fig. S2 of Supporting information. There, the reflections characteristic for ill-crystallized CuO (JCPDS 80-1268) and ZnO (JCPDS 36-1451) phases displaying some overlapping peaks are clearly perceived. The absence of reflections related to Al-containing compounds (including alumina) might be related to the relatively low concentration of Al in the CZA catalyst, though their presence as amorphous material is not discarded [24]. The XRD patterns for the CZA/HZ hybrids (CZA:HZ mass ratio of 2:1) prepared by the different mixing methods are presented in Fig. 1. The XRD pattern of the CZA/HZ(2:1)M sample was simulated from the XRD patterns of the individual CZA and HZ components taking into account the CZA:HZ mass ratio of 2:1. All the hybrids exhibit the characteristic reflections of the MFI crystalline phase besides of those related to the CuO and ZnO phases in the CZA component. It is noteworthy, however, the presence of a Cu–Zn hydrotalcite-like phase $(Cu,Zn)_6Al_2(OH)_{16}CO_3{\cdot}4H_2O$ (JCPDS: 38-0487) in the diffractogram of the hybrid CZA:HZ(2:1)S prepared by the slurry method. This phase is typically observed in the as-prepared CZA precursor (before calcination) together with several mixed metal-hydroxycarbonates such as $(Cu,Zn)_5(CO_3)_2(OH)_6$ (aurichalcite) and

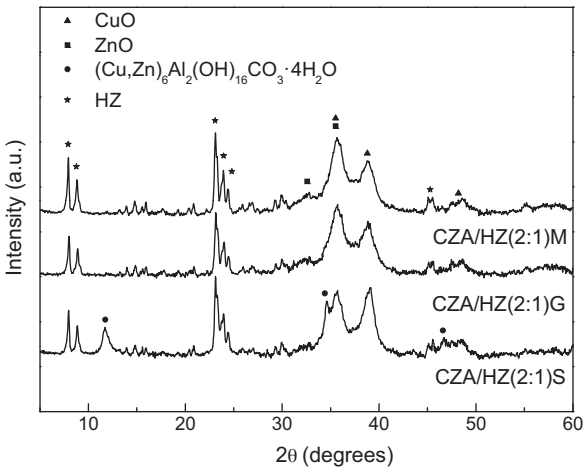

Fig. 1. XRD patterns of hybrid CZA/HZ(2:1) catalysts prepared by different mixing methods. The pattern for the CZA/HZ(2:1)M sample (physical mixture of pre-pelletized components) has been simulated from the individual XRD patterns taking into account the mass ratio between components.

$(Cu,Zn)_2(OH)_2CO_3$ (zincian-malachite or rosasite) which lead, upon thermal decomposition, to the dispersed Cu and Zn oxide phases present in the calcined precursor [27–29]. The contact of the calcined CZA precursor with water during the preparation of CZA:HZ(2:1)S is the likely cause for the partial regeneration of the original Cu–Zn hydrotalcite-like structure (memory effect) assisted by the presence of remaining carbonate anions due to incomplete decomposition of the initial hydroxycarbonate phases during the calcination step. In fact, the same rehydration effect has been shown to occur during the impregnation of a Cu–Zn–Al oxide methanol synthesis catalyst with an aqueous solution of Pd nitrate [29,30]. Besides restoration of the hydrotalcite-like phase, the CuO reflection at ca. 38.8° in the catalyst prepared by the slurry method became more intense and narrower as compared to that in the other two hybrids (Fig. 1), indicating an increase in the average CuO crystallite size. Indeed, by applying the Scherrer's equation to the 38.8° reflection a mean CuO crystallite size of 6.5 nm was obtained for the CZA/HZ(2:1)S sample while it was 5.4 nm for both the CZA oxide precursor (and hence for the hybrid CZA/HZ(2:1)M) and CZA/HZ(2:1)G (grinding method) catalysts (Table 1). Such an increase of ca. 20% in the size of CuO crystallites should lead to a decreased amount of Cu^0 sites (generally believed to be the active sites for methanol synthesis [31,32]) in the H_2-reduced CZA/HZ(2:1)S catalyst. A similar increase in CuO particle size was noticed when the calcined CZA component alone was submitted to the same preparation protocol employed in the slurry method (sample CZAS in Table 1). The increase in the CuO crystallite size upon rehydration of a calcined CZA catalyst has also been reported in the earlier literature to occur in parallel to the partial regeneration of the hydrotalcite-like phase, although a plausible interpretation for such phenomenon was not provided [30].

Table 1 also shows the textural properties of the individual CZA and HZSM-5 components and those of the hybrids prepared by different mixing methods with a CZA:HZ mass ratio of 2:1. The CZA methanol synthesis catalyst displayed a BET area of ca. 98 m^2/g with no microporosity which concur with the values reported for CZA samples prepared by coprecipitation under the same experimental conditions (90–110 m^2/g) [24]. On the other hand, typical BET and micropore volume values of 400 m^2/g and 0.171 mL/g, respectively, were obtained for the commercial HZSM-5 sample (HZ). As seen in the table, the hybrids prepared by the grinding and slurry methods presented BET areas (139–146 m^2/g) and micropore vol-

Table 1
Textural properties of the materials derived from the N_2 adsorption isotherms and CuO crystallite size (from XRD).

Material	BET area (m^2/g)	Micropore area (m^2/g)	Micropore volume (cm^3/g)	$d(CuO)_{XRD}$ (nm)
CZA	98	0	0	5.4
CZAS[a]	65	0	0	6.2
HZ	400	354	0.171	–
CZA/Z(2:1)M	198[b]	118[b]	0.057[b]	5.4
CZA/Z(2:1)G	139 (30%)[c]	88 (25%)[c]	0.042 (26%)[c]	5.4
CZA/Z(2:1)S	146 (26%)[c]	86 (27%)[c]	0.041 (28%)[c]	6.5

[a] CZA catalyst submitted to the same experimental protocol employed in the slurry preparation method.
[b] The values for this hybrid have been calculated from those of the individual CZA and HZ components averaged by their relative mass concentrations.
[c] Values in parenthesis give the % decrease relative to the values calculated for the CZA/HZ(2:1)M catalyst.

umes (0.041–0.042 mL/g) 26–30% lower than those estimated for the CZA/HZ(2:1)M hybrid considering the values of the individual components weighted by their respective mass contributions (BET = 198 m^2/g, V_{micro} = 0.057 mL/g). Since submitting the HZ zeolite alone to the grinding and slurry treatments did not produce noticeable changes in its textural properties, and given that the zeolite has a much higher contribution (2×) than the CZA component to the total area of the hybrids, the decrease in BET and micropore volume observed for CZA/HZ(2:1)G and CZA/HZ(2:1)S catalysts should be mostly attributed to a pore blockage of the zeolite micropores by CZA particles. This fact is supported by the similar relative decrease in BET and micropore volume obtained for these two hybrids, despite a decrease of 33 m^2/g in BET area was noticed upon submitting the CZA component alone to the slurry protocol (sample CZAS) which is consistent with the observed increase in CuO crystallite size for the CZA/HZ(2:1)S hybrid, as discussed before.

The reduction behavior of the CZA component in the different hybrids was studied by H_2-TPR. The corresponding reduction profiles are shown in Fig. 2. The H_2-TPR profile of the single CZA sample (normalized by the mass of CZA in the hybrid) was used as representative for the reduction behavior of the methanol synthesis component in CZA/HZ(2:1)M since this preparation method should preserve the properties of the individual components. As observed in Fig. 2, all three catalysts displayed a similar reduction profile with a main reduction peak in the narrow range of 180–210 °C which is attributed to the reduction of Cu^{2+} to Cu^0 in the CZA component [13,24]. It is noteworthy that an easier reduction of CuO occurs for the CZA/HZ(2:1)G and CZA/HZ(2:1)S hybrids, particularly for the latter displaying the lowest reduction temperature (183 °C). This is somewhat surprising since a higher CuO crystallite size (as observed for CZA/HZ(2:1)S) should, in principle, increase its reduction temperature [24]. A facilitated reduction of

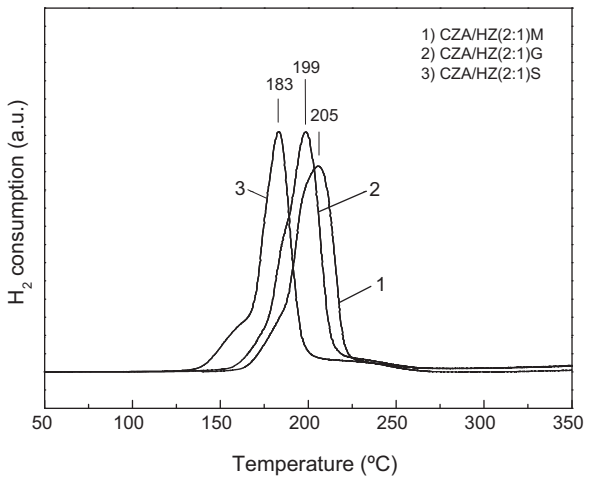

Fig. 2. H_2-TPR profiles for the CZA, CZA/HZ(2:1)S and CZA/HZ(2:1)G samples, normalized to the mass of CZA.

the CuO phase in CZA/zeolite hybrids in comparison to the bare CZA component has also been observed in previous works and ambiguously attributed to a "synergetic effect" arising from interactions between the metallic and acidic functions [10,13]. The same effect could probably explain the slightly lower reduction temperature in CZA/HZ(2:1)G, although the larger temperature shift observed for the catalyst prepared by the slurry method might be an indication of stronger interactions between components in this catalyst. Nonetheless, the observed differences in CuO reducibility are not much relevant and all Cu species in the different hybrids should have been fully reduced after the H_2 reduction treatment at 245 °C applied prior to catalysts. In fact, the measured H_2 consumptions agreed well, within experimental error, with those expected from the real Cu contents and the stoichiometric $Cu^{2+} \rightarrow Cu^0$ reduction.

The acid property of the zeolite has a strong impact on its methanol dehydration activity and hence on the overall STD performance. Here, the acidity of the zeolite in the different hybrids has been studied by infrared spectroscopy coupled with the adsorption of pyridine and desorption at 250 °C. In order to better appraise the changes in acidity that might have occurred during the preparation of catalysts, the IR-pyridine experiments were carried out on hybrid catalysts prepared with a higher zeolite concentration (CZA:HZ mass ratio of 1:2). The IR spectra in the pyridine vibration region for the bare HZ zeolite and the hybrids prepared by the grinding and slurry methods are shown in Fig. 3. For comparison purposes, the spectra were normalized by weight of zeolite. Thus, the normalized IR spectrum for HZ may be taken as representative for the zeolite in the CZA/HZ(1:2)M hybrid for which the original characteristics of the metallic and acid components should have been retained. The spectrum of the bare HZ zeolite exhibited the characteristic IR bands at 1455, 1612, and 1621 cm^{-1} attributed to pyridine interacting with Lewis acid sites, as well as the bands at 1547 and 1636 cm^{-1} assigned to pyridine chemisorbed on Brønsted acid sites. The signal at 1490 cm^{-1} is associated to pyridine retained on both Brønsted and Lewis acid sites [33]. It is remarkable that the intensity of the signal at 1455 cm^{-1}, which is typically related to Lewis acid sites associated to extra-framework Al (EFAL) species [34], is very low in HZ. This fact agrees well with the very minor contribution from non-framework Al^{VI} and Al^{V} species observed in the ^{27}Al MAS NMR spectrum of this commercial zeolite (Fig. S3, Supporting information). Interestingly, significant differences in the acid properties of the zeolite in the hybrids prepared by the grinding and slurry methods with respect to the bare HZ are evidenced in Fig. 3. Thus, a large increase in the amount of Lewis acid sites and a significant reduction in Brønsted acidity were noticed for the zeolite in the two hybrids as compared to the bare HZ sample. The quantitative acidity data derived from the IR-pyridine measurements are given in Table 2. As seen there (and also inferred from the respective spectra in Fig. 3), the reduction in Brønsted acidity was more drastic for the zeolite in the hybrid prepared by the slurry approach while, surprisingly, the Lewis acidity increased to a larger extent for the zeolite in the hybrid obtained by the grinding method. It is worth mentioning that a large increase in the amount of Lewis acid

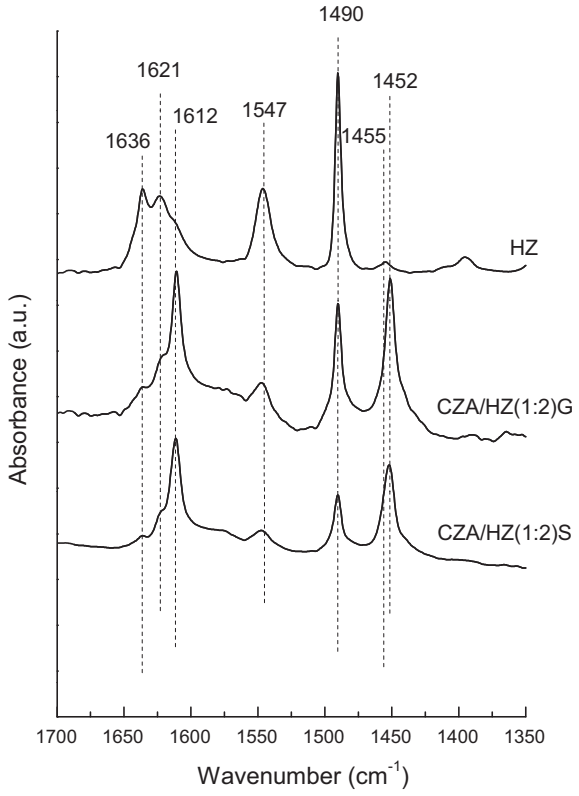

Fig. 3. IR spectra in the pyridine region for the bare HZSM-5 zeolite (HZ) and CZA/HZ(1:2)G and CZA/HZ(1:2)S hybrid catalysts. For comparison purposes the spectra have been normalized to the mass of zeolite.

sites and suppression of Brønsted acidity has been already observed by Flores et al. for hybrid CuZn(Al)-ferrierite catalysts prepared by coprecipitation–sedimentation and coprecipitation–impregnation methods [21]. According to these authors, the reduction in the Brønsted acidity for the zeolite in the hybrids was attributed to the partial blockage of acid sites by the methanol synthesis catalyst while the increase in Lewis acidity was tentatively related to the creation of new sites by the Al present in the CZA catalyst without giving further insights. In our study, a slight shift of the Lewis band towards lower wavenumbers (from 1455 to 1452 cm^{-1}) for the zeolite in the two hybrids as compared to the bare HZ sample was noticed besides the increase in band intensity (Fig. 3). This fact might indicate that the newly developed Lewis acid sites in the hybrids could be different in nature to those associated to EFAL species in the bare zeolite. At this point we may hypothesize that the new Lewis acid sites created in the hybrid catalysts as well as the large reduction in Brønsted acidity could be originated from the exchange of zeolite protons with Cu^{2+} and/or Zn^{2+} cations from the CZA catalyst as a consequence of CZA–zeolite interactions occurring during the catalyst preparations. Indeed, the partial exchange of H^+ in HZSM-5 with either Cu^{2+} or Zn^{2+} cations has been shown to produce new Lewis acid sites characterized by an IR-pyridine band peaking at 1452 cm^{-1} besides the concomitant reduction in

Table 2
Acidity results for the bare HZ zeolite and the CZA/HZ hybrids normalized by mass of zeolite, as determined by FTIR-pyridine after desorbing the base probe at 250 °C.

Sample	Amount of acid sites ($\mu mol/g_{zeolite}$)	
	Brønsted	Lewis
HZ	174	8
CZA/HZ(1:2)G	52	200
CZA/HZ(1:2)S	22	125

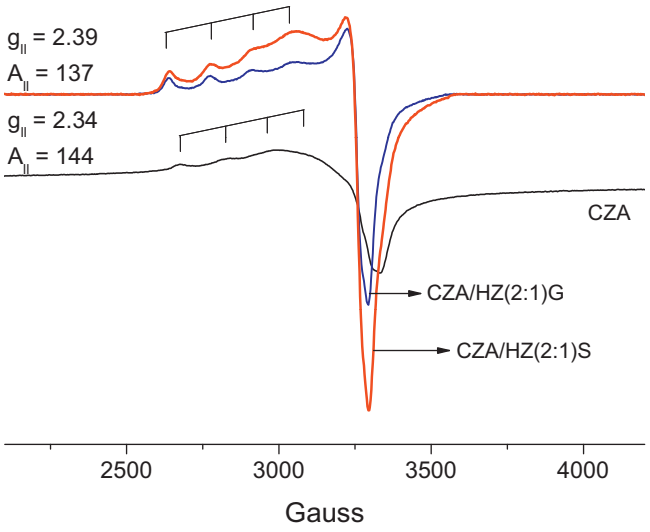

Fig. 4. EPR spectra for the CZA catalyst and CZA/HZ(2:1)G and CZA/HZ(2:1)S hybrids.

the amount of Brønsted acid sites [35,36]. At present, however, we cannot provide a plausible interpretation for the lower amount of both Brønsted and Lewis acid sites in the hybrid prepared by the slurry method as compared to that obtained by grinding (Table 2). The fact that the zeolite in these two hybrids displayed a similar microporosity (Table 1) rules out differences in the extent of zeolite pore blockage by the Cu-based catalyst as the origin of the differences in acidity trends.

In order to support the above hypothesis of inter-cationic exchange between components (at least for Cu cations) as the likely cause for the reduction in zeolite Brønsted acidity and increase in the concentration of Lewis acid sites, the bare CZA catalyst and the two hybrids prepared by grinding and slurry methods were characterized by electron paramagnetic resonance (EPR) spectroscopy as detailed in Section 2. EPR has been extensively applied to characterize isolated Cu^{2+} species in Cu-exchanged zeolites, and particularly in Cu–ZSM-5 [37–40]. The EPR spectra for the calcined CZA precursor and the two hybrids (CZA:HZ mass ratio of 2:1) are presented in Fig. 4. The spectrum for CZA shows a broad band at $g \approx 2$ and $\Delta H_{pp} = 2000$ G plus other axially symmetric signal with resolved hyperfine coupling ($g_{||} = 2.34$ and $A_{||} = 144$ G) as it can be better appraised in Fig. S4 of Supporting information. The broad band presents no paramagnetic behavior, as the intensity does not increase when temperature decreases. The axially symmetric signal is assigned to isolated copper species interacting with close Al^{3+} ions, as proposed earlier [41]. The amount of such isolated species was determined to be 1.00% of the total amount of Cu present in the material, indicating that most of the Cu species in the CZA component are EPR-silent as expected from the existence of strong magnetic interactions between Cu^{2+} ions in CuO crystallites [42,43].

On the other hand, the EPR spectra of hybrid CZA/HZ(2:1)G and CZA/HZ(2:1)S catalysts mainly consisted of an axially symmetric signal with well resolved hyperfine coupling in the parallel region, with parameters $g_{||} = 2.39$ and $A_{||} = 137$ G (Fig. 4). These parameters are characteristic of isolated Cu^{2+} species in exchange positions of hydrated Cu–ZSM-5 zeolites [37,38]. This result, thus, confirms that the exchange of zeolite H^+ by Cu^{2+} ions does indeed occurs during the preparation of the hybrids by the grinding and slurry methods. In order to estimate the amounts of exchanged isolated Cu^{2+} species in the two hybrids, quantification of the resolved axially symmetric signals in the range of 2500–3750 G was performed by double integration of the respective EPR spectrum after subtraction of the wide signal from the CZA component as noted above ($g \approx 2$ and $\Delta H_{pp} = 2000$ G). The results revealed that 0.36 and 0.22 wt% of

the total amount of Cu occupied exchange positions in the zeolite for the CZA/HZ(2:1)S and CZA/HZ(2:1)G samples, respectively, thus indicating a higher extent of Cu^{2+} exchange for the zeolite in the hybrid prepared by the slurry method. This result is consistent with the larger decrease in Brønsted acidity observed by IR-pyridine for the CZA/HZ(1:2)S sample as compared to CZA/HZ(1:2)G. Nevertheless, it has to be kept in mind that the EPR and IR-pyridine characterizations do not exclude the presence of exchanged Zn^{2+} species which might also contribute to the acidity trends previously discussed.

Though a definite mechanistic interpretation for the migration of cationic species from the CZA component to the zeolite during the preparation of the hybrids is not possible at this stage, it is likely that in the case of the slurry method it would involve the partial dissolution of the metal cations in water and their further exchange by protons in the zeolite when both components are slurried together. For the grinding method the process could well proceed through the so-called *contact-induced ion exchange* mechanism [44–46]. This mechanism was proposed in order to account for the observed exchange of cationic species between different zeolites upon a simple physical contact between the crystallites [44], and is believed to be mediated by water filling the micropores in hydrated zeolite [47]. The *contact-induced ion exchange* mechanism was also invoked to explain the exchange of Li^+ with Na^+ occurring upon grinding a mechanical mixture of hydrated NaY zeolite and crystalline LiCl salt [46].

The presented characterization results clearly showed that interactions between the CZA and zeolite components take place during the preparation of the hybrid STD catalysts by the slurry and grinding methods. Such interactions involve, on one hand, partial blockage of zeolite micropores by the CZA component and, on the other hand, migration of Cu^{2+} species (and possibly also Zn^{2+}) from the CZA catalyst to the zeolite and their exchange with protons. The consequences of the CZA–zeolite interactions on the methanol synthesis and methanol dehydration activities in the context of the direct syngas-to-DME process will be discussed in the next sections.

3.2. Catalytic results

3.2.1. Methanol synthesis reaction

Prior to assessing the impact of the CZA–zeolite interactions on the activity of the methanol synthesis catalyst, it would be interesting to evaluate first whether or not the activity of the CZA catalyst for the methanol synthesis reaction is altered during the slurry and grinding preparations for hybrids comprising an acid-free zeolite (thus lacking ion exchange capacity). For this purpose, CZA/silicalite-1 samples (CZA:S1 mass ratio of 2:1) were obtained by the same methods applied for preparing the CZA/HZ hybrids, as detailed in Section 2.

The results of the syngas conversion over the CZA/S1 samples at the typical STD reaction conditions (260 °C, 4 MPa, 15.0 $L_{syngas}\ g_{cat}^{-1}\ h^{-1}$) are shown in Table 3. As seen there, nearly the same CO conversion of ca. 25% was achieved for the samples prepared by the mixture of individual pellets (CZA/S1(2:1)M) and by grinding the mixture of powders (CZA/S1(2:1)G). By contrast, the mixture prepared by the slurry method (CZA/S1(2:1)S) lead to a lower conversion of ca. 22%, indicating that the CZA component in this catalyst is slightly less active for methanol synthesis. This result can be explained by the increase in CuO crystallite size (and concomitant decrease in surface area) observed when the CZA precursor was contacted with water in the slurry solution (Table 1) which obviously lowers the amount of active Cu sites available for the syngas-to-methanol reaction. Previous studies have also evidenced a direct relationship between Cu surface area and methanol synthesis activity [24,48]. As observed in Table 3, methanol was the main reaction product for all three CZA/S1 catalysts with 97–98% selectivity. On the other hand, DME, other oxygenates, and hydrocarbons were formed in very low amounts with selectivities of 0.1%, 0.4–0.6%, and 0.3–0.4%, respectively, as expected from the lack of acid sites in these mixtures. In fact, these products were shown to form in low amounts during the methanol synthesis on Cu-based catalysts and attributed to the presence of metal impurities and/or to weak surface acid sites [49,50]. Finally, minor differences in CO_2 selectivity are observed for the different samples in Table 3 (1.0–1.9%) suggesting that the method of preparation did not much alter the WGS activity of the Cu catalyst.

Further, the impact of the preparation method on the methanol synthesis activity of the CZA component was also assessed using bifunctional CZA/HZ catalysts with an "excess" of acid sites (CZA:HZ mass ratio of 2:1) and thus under methanol synthesis-controlled STD conditions. The influence of GHSV (at 260 °C and 4 MPa) on CO conversion and DME yield is shown in Fig. 5. At the lowest GHSV value of 1.7 $L_{syngas}\ g_{cat}^{-1}\ h^{-1}$ all the catalysts display almost the same CO conversion (89%) close to the predicted thermodynamic conversion under the studied conditions (ca. 93%). Therefore, it was necessary to evaluate the activity at higher GHSV so as to attain conversions well below the thermodynamic value. At GHSV of 5.1 and 8.5 $L_{syngas}\ g_{cat}^{-1}\ h^{-1}$ no appreciable differences in activity were still observed for the CZA/HZ(2:1)M and CZA/HZ(2:1)G hybrids while a slightly lower CO conversion was attained for the hybrid prepared by the slurry method (Fig. 5a). Similar trends were found for the DME yields (Fig. 5b). The catalytic results for the three hybrid catalysts at variable GHSV are summarized in Table S1 of Supporting information. As it can be seen there, no major differences in product selectivity between the hybrids were noticed at the lowest GHSV of 1.7 $L_{syngas}\ g_{cat}^{-1}\ h^{-1}$. At increasing GHSV values the catalyst prepared as mixture of pre-pelletized components displayed a slightly higher DME selectivity (in detriment of MeOH).

Therefore, it is concluded from the above two sets of experiments that the methanol synthesis activity of the CZA catalyst is slightly reduced when the hybrid catalyst is prepared by the slurry method due to an increase in CuO crystallite size while the grinding method has practically no effect on the CZA activity. In the following section, the influence of the mixing method on the zeolite dehydration activity will be analyzed.

3.2.2. Methanol dehydration reaction

In order to evaluate whether the different mixing methods might have altered the intrinsic dehydration activity of the HZSM-5 zeolite or not, the parent HZ sample was submitted to the grinding (sample HZG) and slurry (sample HZS) conditions and then tested for methanol dehydration at the STD temperature of 260 °C using pure methanol as feed, as detailed in Section 2.3.1. The obtained methanol dehydration rates were 262, 257, and 266 $\mu mol\ g^{-1}\ s^{-1}$ for the HZ, HZG, and HZS samples, respectively. These results clearly show that the grinding and slurry conditions have, by themselves, no affect on the intrinsic dehydration activity of the HZSM-5 zeolite. Therefore, any change in dehydration activity that may occur during the STD experiments (under methanol dehydration-controlled conditions) should be exclusively related to the interactions between the components arising during the preparation of the CZA/HZ hybrids.

Due to the high dehydration activity of the HZSM-5 zeolite, relatively high CZA:zeolite mass ratios had to be used in order to run the STD experiments under methanol dehydration-controlled conditions. In fact, for the typical CZA:HZ mass ratio of 2:1 all the three hybrid catalysts displayed nearly the same CO conversion (ca. 89%) and DME yield (ca. 58%) approaching the values dictated by the thermodynamic equilibrium under the applied conditions (93% CO conversion and 64% DME yield). Therefore, hybrids with CZA:HZ mass ratios of 3:1 and 6:1 were prepared. The STD results

Table 3
Methanol synthesis tests for CZA/S1(2:1)M, CZA/S1(2:1)G, and CZA/S1(2:1)S mixtures comprising acid-free silicalite-1 (S1). Reaction conditions: 260 °C, 4.0 MPa, 15.0 $L_{syngas}\ g_{cat}^{-1}\ h^{-1}$, TOS = 3 h.

Sample	CO conv. (%)	Selectivity (%C)				
		MeOH	CO_2	DME	Other oxyg.[a]	HC[b]
CZA/S1(2:1)M	24.8	97.1	1.9	0.1	0.6	0.3
CZA/S1(2:1)G	24.7	97.5	1.4	0.1	0.6	0.4
CZA/S1(2:1)S	21.7	98.2	1.0	0.1	0.4	0.3

[a] Other oxygenates: mostly EtOH and other higher alcohols in lower amounts.
[b] HC, hydrocarbons.

Table 4
STD experiments under methanol dehydration-controlled conditions: T = 260 °C, P = 4 MPa, GHSV = 1.7 $L_{syngas}\ g_{cat}^{-1}\ h^{-1}$, TOS = 3 h.

Catalyst	CO conversion (%)	Selectivity (%C)				DME yield (%C)	DME productivity (g_{DME}/kg_{cat} h)
		DME	MeOH	CO_2	HC		
CZA/HZ(3:1)M	89.2	63.6	4.2	31.9	0.3	56.7	265.3
CZA/HZ(3:1)G	67.2	44.7	28.2	25.5	1.4	30.0	140.5
CZA/HZ(3:1)S	59.2	39.7	36.5	22.4	1.2	23.5	109.9
CZA/HZ(6:1)M	87.9	64.1	4.5	31.2	0.2	56.3	263.5
CZA/HZ(6:1)G	51.0	22.5	53.5	19.6	2.4	11.5	53.7
CZA/Z(6:1)S	42.6	9.1	73.3	13.3	1.9	3.9	18.1
CZA/HZ(9:1)M	89.4	63.7	4.4	31.7	0.2	56.9	266.3
Therm. eq.[a]	92.9	69.0	4.8	26.1	–	64.1	–

[a] Thermodynamic equilibrium values were calculated by Aspen Hysys, using ΔG of the main reactions involved in the STD process.

for these hybrids are shown in Table 4. As observed, significantly lower CO conversions and DME yields were attained for the catalysts prepared by grinding and slurry methods as compared to that obtained by the mixing of individual pellets, for which no interactions between components are expected to occur. The differences became larger at higher CZA:HZ ratios. Interestingly, the results in Table 4 show that the activity and selectivity of the latter catalyst hardly changed with the increase in CZA:HZ mass ratio keeping values close to the equilibrium even for ratios as high as 9:1. It is also seen that the catalysts prepared by this simple approach were those leading to the highest DME productivities (ca. 265 g_{DME}/kg_{cat} h). Moreover, it is also noticed that the hybrid prepared by the slurry method was less efficient for producing DME from syngas than that obtained by grinding, particularly at the higher CZA:HZ mass ratio of 6:1. The decrease in CO conversion as well as the increase in MeOH selectivity (and concomitant decrease in DME selectivity) experienced by the catalysts prepared by grinding and slurry methods are clear consequences of a decreased methanol dehydration ability for the zeolites in these two hybrids and can be well accounted for by taking into consideration the coupling between the main reactions involved in the STD process, as discussed in the Introduction.

The above trends confirm that for CZA:HZ mass ratios of 3:1 and higher the overall STD process is indeed controlled by the dehydration of methanol on the zeolite acid sites. By comparing these results with those of pure methanol dehydration experiments previously discussed, it can be concluded that the dehydration activity of the HZSM-5 zeolite was negatively impacted by detrimental interactions emerging during the preparation of hybrids by the grinding and, particularly, the slurry methods. According to the characterization results presented in this study, such detrimental interactions involve a partial blockage of the zeolitic micropores by the CZA particles as well as a partial exchange of the zeolite protons by Cu^{2+} (and possibly Zn^{2+}) cations from the CZA component. Both kinds of interactions will certainly contribute to the decrease in the amount of accessible Brønsted acid sites (as detected by IR-pyridine) and thus to the lower methanol dehydration activity of the zeolites in the hybrids obtained by the grinding and slurry methods. An indirect conclusion from these results is that the newly created Lewis acid sites associated to the exchanged metal cations do not significantly contribute to the overall zeolite dehydration activity. Nevertheless, the existence of other type of interactions cannot be discarded from the results presented here and will be worth to be studied in future works.

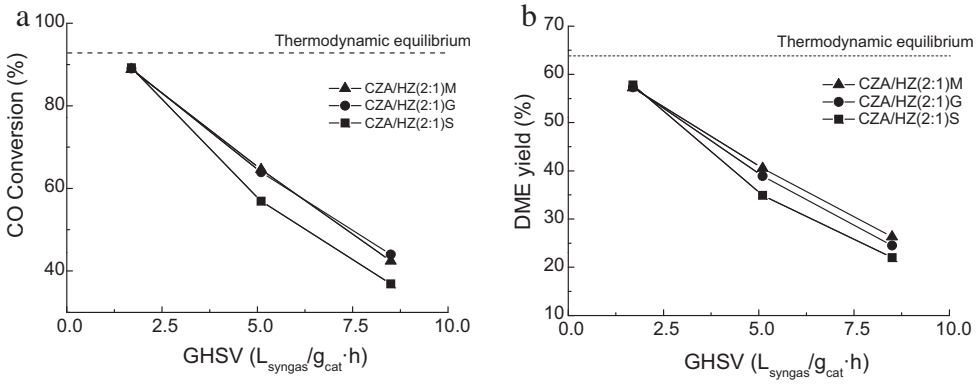

Fig. 5. Change of CO conversion (a) and DME yield (b) with GHSV for CZA/HZ hybrids (CZA:HZ mass ratio of 2:1) under methanol synthesis-controlled conditions: 260 °C, 4 MPa.

4. Conclusions

The catalytic properties of hybrid CZA/HZ catalysts for the one-step DME synthesis (STD process) became significantly affected by the particular method applied for preparing the mechanical mixtures. Thus, CZA/HZ hybrids obtained by grinding and slurrying together the respective component powders lead to detrimental interactions between the components that significantly reduced their efficiency for the STD reaction as compared to hybrids obtained by a simple physical mixture of the individual pellets and thus having no chance for interactions.

In the case of the hybrid prepared by the slurry approach, the contact of the CZA oxide precursor with water provoked structural changes (restoration of the original hydrotalcite-like $(Cu,Zn)_6Al_2(OH)_{16}CO_3{\cdot}4H_2O$ phase) and an increase in the CuO crystallite size leading to a lower activity for methanol synthesis. No major changes in the physicochemical and catalytic properties of the CZA component occurred for the hybrid prepared by the grinding method. On the other hand, submitting the HZSM-5 zeolite (in the absence of the CZA catalyst) to the grinding and slurry conditions did not alter its intrinsic methanol dehydration activity, as verified by independent catalytic experiments using pure methanol as feed. By contrast, the contact of the zeolite with CZA during the grinding and slurry preparations produced a significant deterioration in the textural and acidic properties of the zeolite that negatively impacted its methanol dehydration activity and consequently the efficiency of the corresponding CZA:HZ hybrids for the syngas-to-DME reaction. The origin of such detrimental interactions is twofold. On one hand, the partial blockage of the zeolite micropores by CZA particles and, on the other hand, the partial exchange of zeolite protons by Cu^{2+} (and possibly also Zn^{2+}) cations, both factors producing a significant reduction in the amount of Brønsted acid sites available for dehydrating methanol to DME. The presence of isolated Cu^{2+} species occupying exchange positions in HZSM-5 zeolite as a consequence of the physical contact between the CZA and zeolite components was unambiguously evidenced, for the first time, using EPR spectroscopy. The inter-cation exchange effect was seen to be more pronounced for the hybrid prepared by the slurry approach.

Based on previous studies, it can be suggested that in the case of the catalyst prepared by the slurry method the process probably occurs through the partial dissolution of the metal cations in water while for the grinding method the previously reported *contact-induced ion exchange* mechanism is likely. Nevertheless, the possibility for other kinds of interactions arising during the preparation of hybrid STD catalysts cannot be ruled out. The STD catalytic results clearly revealed that the most efficient hybrid catalyst is that prepared by the simple mixing of pre-pelletized components for which the properties of the two catalytic functions are preserved. In this way, very active catalysts producing DME yields of ca. 58% (ca. 90% of the thermodynamic equilibrium yield at the studied STD conditions), were produced even at CZA:HZSM-5 mass ratios as high as 9:1.

Acknowledgments

Financial support by the Comisión Interministerial de Ciencia y Tecnología (CICYT) of Spain through the Project CTQ2010-17988/PPQ is gratefully acknowledged. A. García-Trenco thanks the Ministerio de Ciencia e Innovación (MICINN) of Spain for a predoctoral (FPI) scholarship.

Appendix A. Supplementary data

Supplementary data associated with this article can be found, in the online version, at doi:10.1016/j.cattod.2011.06.034.

References

[1] W.W. Kaeding, S.A. Butter, J. Catal. 61 (1980) 155–164.
[2] G. Cai, Z. Liu, R. Shi, C. He, L. Yang, C. Sun, Y. Chang, Appl. Catal. A 125 (1995) 29–38.
[3] T.A. Semelsberger, R.L. Borup, H.L. Greene, J. Power Sources 156 (2006) 497–511.
[4] N. Inoue, Y. Ohno, Petrotech 24 (2001) 319–322.
[5] J. Topp-Jorgense, US Patent 4,536,485 (1985), to Haldor Topsoe A/S, Denmark.
[6] J.B. Hansen, F.H. Joensen, H.F.A. Topsoe, US Patent 5,189,203 (1993), to Haldor Topsoe A/S, Denmark.
[7] J.H. Kim, M.J. Park, S.J. Kim, O.S. Joo, K.D. Jung, Appl. Catal. A 264 (2004) 37–41.
[8] L. Wang, Y. Qi, Y. Wei, D. Fang, S. Meng, Z. Liu, Catal. Lett. 106 (2006) 61–66.
[9] D. Mao, W. Yang, J. Xia, B. Zhang, Q. Song, Q. Chen, J. Catal. 230 (2005) 140–149.
[10] Q. Ge, Y. Huang, F. Qiu, S. Li, Appl. Catal. A 167 (1998) 23–30.
[11] J.L. Li, X.G. Zhang, T. Inui, Appl. Catal. A 147 (1996) 23–33.
[12] F.S. Ramos, A.M. Duarte de Farias, L.E.P. Borges, J.L. Monteiro, M.A. Fraga, E.F. Sousa-Aguiar, L.G. Appel, Catal. Today 101 (2005) 39–44.
[13] G.R. Moradi, M. Nazari, F. Yaripour, Fuel Process. Technol. 89 (2008) 1287–1296.
[14] P.S.S. Prasad, J.W. Bae, S.H. Kang, Y.J. Lee, K.W. Jun, Fuel Process. Technol. 89 (2008) 1281–1286.
[15] S.H. Kang, J.W. Bae, K.W. Jun, H.S. Potdar, Catal. Commun. 9 (2008) 2035–2039.
[16] K.S. Yoo, J.H. Kim, M.J. Park, S.J. Kim, O.S. Joo, K.D. Jung, Appl. Catal. A 330 (2007) 57–62.
[17] D. Song, W. Cho, D.K. Park, E.S. Yoon, J. Ind. Eng. Chem. 13 (2007) 815–826.
[18] G.R. Moradi, S. Nosrati, F. Yaripor, Catal. Commun. 8 (2007) 598–606.
[19] S.P. Naik, H. Du, H. Wan, V. Bui, J.D. Miller, W.W. Zmierczak, Ind. Eng. Chem. Res. 47 (2008) 9791–9794.
[20] X.D. Peng, B.A. Toseland, R.P. Underwood, Stud. Surf. Sci. Catal. 111 (1997) 175–182.
[21] J.H. Flores, M.I. Pais da Silva, Colloids Surf. A 322 (2008) 113–123.
[22] J.H. Flores, G. Solórzano, M.I. Pais da Silva, Appl. Surf. Sci. 254 (2008) 6461–6466.
[23] T. Takeguchi, K. Yanagisawa, T. Inui, M. Inoue, Appl. Catal. A 192 (2000) 201–209.
[24] C. Baltes, S. Vukojević, F. Schüth, J. Catal. 258 (2008) 334–344.
[25] W. Song, R.E. Justice, C.A. Jones, V.H. Grassian, S.C. Larsen, Langmuir 20 (2004) 4696–4702.
[26] C.A. Emeis, J. Catal. 141 (1993) 347–354.
[27] K. Klier, Adv. Catal. 31 (1982) 243–313.
[28] J.C.J. Bart, R.P.A. Sneeden, Catal. Today 2 (1987) 1–124.
[29] I. Melián-Cabrera, M. López Granados, J.L.G. Fierro, Catal. Lett. 84 (2002) 153–161.
[30] I. Melián-Cabrera, M. López-Granados, J.L.G. Fierro, J. Catal. 210 (2002) 273–284.
[31] K.C. Waugh, Catal. Today 15 (1992) 51–75.
[32] P.B. Rasmussen, M. Kazuta, Y. Chorkendorff, Surf. Sci. 318 (1994) 267–280.
[33] G. Busca, Phys. Chem. Chem. Phys. 1 (1999) 723–736.
[34] S.M. Campbell, D.M. Bibby, J.M. Coddington, R.F. Howe, R.H. Meinhold, J. Catal. 161 (1996) 338–349.
[35] J. Connerton, R.W. Joyner, M. Padleyt, J. Chem. Soc. Faraday Trans. 91 (1995) 1841–1844.
[36] H. Berndt, G. Lietz, B. Liicke, J. Vijlter, Appl. Catal. A 146 (1996) 351–363.
[37] M.H. Groothaert, K. Pierloot, A. Delabie, R.A. Schoonheydt, Phys. Chem. Chem. Phys. 5 (2003) 2135–2144.
[38] M. Anderson, L. Kevan, J. Phys. Chem. 91 (1987) 4174–4179.
[39] J. Dedezek, Z. Sobalik, Z. Tvaruzkova, D. Kaucky, B. Wichterlova, J. Phys. Chem. 99 (1995) 16327–16337.
[40] S.C. Larsen, A. Aylor, A.T. Bell, J.A. Reimer, J. Phys. Chem. 98 (1994) 11533–11540.
[41] S. Velu, K. Suzuki, M. Okazaki, M.P. Kapoor, T. Osaki, F. Ohashi, J. Catal. 194 (2000) 373–384.
[42] R.T. Figueiredo, A. Martínez-Arias, M. López Granados, J.L.G. Fierro, J. Catal. 178 (1998) 146–152.
[43] F. Mehran, S.E. Barnes, G.V. Chandrashekhar, T.R. McGuire, M.W. Shafer, Solid State Commun. 67 (1988) 1187–1189.
[44] C.A. Fyfe, G.T. Kokotailo, J.D. Graham, C. Browning, G.C. Gobbi, M. Hyland, G.J. Kennedy, C.T. DeSchutter, J. Am. Chem. Soc. 108 (1986) 522–523.
[45] G. Borbély, H.K. Beyer, L. Radics, P. Sándor, Zeolites 9 (1989) 428–431.
[46] B. Sulikowski, G. Borbély, H.K. Beyer, H.G. Karge, I.W. Mishin, J. Phys. Chem. 93 (1989) 3240–3243.
[47] H.G. Karge, H.K. Beyer, Solid-state ion exchange in microporous and mesoporous materials , in: H.G. Karge, J. Weitkamp (Eds.), Molecular Sieves, vol. 3, Springer, Berlin, 2002, pp. 43–201.
[48] D. Jingfa, S. Qi, Z. Yulong, C. Songying, W. Dong, Appl. Catal. A 139 (1996) 75–85.
[49] X.M. Liu, G.Q. Lu, Z.F. Yan, J. Beltramini, Ind. Eng. Chem. Res. 42 (2003) 6518–6530.
[50] A.M. Hilmen, M. Xu, M.J.L. Gines, E. Iglesia, Appl. Catal. A 169 (1998) 355–372.